coatings

MDPI

Article

Study on the Influence of Modified Steel Slag Filler on the Rheological Properties and Moisture Stability of Asphalt Mastic

Zhe Ma [1,2], Chao Pu [3,4,*], Guanghui Zhang [1,2], Bin Wang [3,4], Waiitii Litifu [1,*], Chunmei Liu [5], Sihua Li [6] and Peng Yin [7,*]

1 Xinjiang Communications Investment Construction Management Co., Ltd., Urumqi 830000, China; mazhe2560@126.com (Z.M.); zhangguanghui1245@163.com (G.Z.)
2 Xinjiang Awu'a Highway Development Co., Ltd., Urumqi 830000, China
3 Xinjiang Transport Planning Survey and Design Institute Co., Ltd., Urumqi 830000, China; xj11992023@163.com
4 Xinjiang Key Laboratory for Safety and Health of Transportation Infrastructure in Alpine and High-Altitude Mountainous Areas, Urumqi 830000, China
5 Xinjiang Transportation Investment (Group) Co., Ltd., Urumqi 830000, China; 17767680324@163.com
6 Xinjiang Uygur Autonomous Region Road Traffic Emergency Equipment and Materials Reserve Center, Urumqi 830000, China; 18199866405@163.com
7 School of Infrastructure Engineering, Dalian University of Technology, No. 2, Linggong Road, Ganjingzi District, Dalian 116024, China
* Correspondence: puchao19950906@163.com (C.P.); wayit_litip@163.com (W.L.); yp2021@mail.dlut.edu.cn (P.Y.)

Abstract

Steel slag is a major solid waste generated by the steelmaking industry. Its characteristics, including high hardness and large specific surface area, offer the potential to replace traditional mineral fillers in asphalt mixtures. However, the high alkalinity of unmodified steel slag often leads to unbalanced rheological properties and insufficient moisture stability in asphalt mastic. In this study, a modified steel slag filler was prepared using a process involving crushing and screening, water washing for dealkalization, and surface modification with a silane coupling agent. Using limestone powder and hydrated lime as control groups, the modification effects on base asphalt mastic were systematically investigated. Rheological properties were characterized using a dynamic shear rheometer (DSR) and bending beam rheometer (BBR). Interfacial performance was evaluated through pull-off tests and water immersion dispersion tests. Furthermore, mechanisms were elucidated using X-ray Fluorescence (XRF), BET specific surface area analysis, and surface free energy (SFE) tests. The results indicate that the modified steel slag significantly enhances the high-temperature deformation resistance of the asphalt mastic. At 58 °C, the complex modulus reached 7.3 MPa, representing increases of 43.3% compared to limestone powder mastic. At −18 °C, the creep stiffness increased by only 3.0%, suggesting that low-temperature cracking resistance remained fundamentally stable. The water immersion dispersion loss rate was 2.12%, and the attenuation rate of pull-off strength after water immersion was 12.5%, indicating that its resistance to moisture damage is superior to that of limestone powder and comparable to that of hydrated lime. Mechanism analysis reveals that the large specific surface area of the modified steel slag strengthens physical adsorption, while the basic oxides undergo a weak acid–base reaction with the acidic components of the asphalt. Additionally, surface modification improves compatibility. The preparation process for modified steel slag is simple; it can be used as a standalone substitute for traditional mineral fillers, balancing both performance and environmental benefits.

Check for updates

Academic Editor: Valeria Vignali

Received: 31 January 2026
Revised: 26 February 2026
Accepted: 4 March 2026
Published: 9 March 2026

Copyright: © 2026 by the authors. Licensee MDPI, Basel, Switzerland. This article is an open access article distributed under the terms and conditions of the Creative Commons Attribution (CC BY) license.

Keywords: modified steel slag; asphalt mastic; rheological properties; moisture stability; action mechanism

1. Introduction

Due to their superior ride quality and the ease of construction and maintenance, asphalt mixtures have become the most widely applied pavement materials in highway engineering in China [1,2]. As the core binding phase of asphalt mixtures, asphalt mastic is composed of asphalt binder and mineral filler mixed in specific proportions; its performance directly dictates critical pavement properties, including high-temperature rutting resistance, low-temperature cracking resistance, and moisture stability [3]. Specifically, rheological properties serve as the primary characterization of the viscoelastic behavior of asphalt mastic, while high-temperature rheological parameters govern cracking resistance [4]. Consequently, optimizing the rheological properties of asphalt mastic is a critical approach to mitigating early-stage pavement distresses.

As a critical component of asphalt mastic, mineral filler accounts for only 6–10% of the mixture by mass but contributes over 75% of the total specific surface area; consequently, its physicochemical properties exert a decisive influence on the structure and performance of the mastic [5]. Traditional asphalt mixtures predominantly employ limestone powder as filler. However, the extraction of limestone entails significant natural resource consumption, and its reinforcement effect on high-temperature rheology is limited, making it difficult to meet the performance requirements of pavements subjected to heavy traffic loads and extreme climatic conditions [6]. Concurrently, China's steelmaking industry generates hundreds of millions of tons of steel slag annually [7]. This massive amount of industrial solid waste is typically disposed of via open-air stockpiling, which not only occupies vast land resources but also poses severe environmental risks, as high-alkalinity components may leach into soil and groundwater [8]. Rich in components such as CaO and Fe_2O_3, steel slag is characterized by high hardness and a large specific surface area. Theoretically, it possesses significant potential to replace traditional mineral powder as an asphalt filler. This application not only offers a novel pathway for the resource utilization of steel slag but also reduces the cost of pavement materials, aligning with the environmental development orientation under the Dual Carbon policy [9].

In recent years, scholars both domestically and internationally have conducted preliminary explorations into the application of steel slag in asphalt materials. Studies have indicated that the incorporation of steel slag can enhance the viscosity and deformation resistance of asphalt mastic; however, its high alkalinity and strong hydrophilicity often lead to insufficient moisture stability, making the mastic prone to interfacial stripping upon water immersion [9,10]. Other research has confirmed that the specific surface area of steel slag is a key factor influencing the rheological properties of the mastic, yet effective modification schemes addressing the high alkalinity issue remain lacking [11]. Significant gaps persist in existing research: the high alkali content (e.g., Na_2O, CaO) of unmodified steel slag is susceptible to reacting with the acidic components of asphalt to generate water-soluble products, thereby exacerbating the risk of moisture damage and causing an imbalance between rheological properties and moisture stability [12,13]. Furthermore, most studies focus on basic performance evaluations and lack a systematic characterization of rheological properties, often relying on complex microscopic instruments such as fourier transform infrared spectroscopy (FTIR) and atomic force microscopy (AFM) for mechanism analysis, which hinders widespread engineering application [14,15]. The correlation between the steel slag modification process and the enhancement of rheological perfor-

mance remains unclear, restricting its large-scale utilization [16,17]. Additionally, existing modification technologies tend to focus on optimizing a single performance metric, failing to achieve synergy among high-temperature rheological reinforcement, the preservation of low-temperature cracking resistance, and the enhancement of moisture stability [18,19].

To address the issues, this study proposes a simple preparation process for modified steel slag filler involving crushing and screening, water washing for dealkalization, and surface modification with a silane coupling agent. The performance of asphalt mastic containing this filler was investigated using limestone powder and hydrated lime as control groups. The study aims to optimize the modification process to reduce alkalinity and enhance compatibility with asphalt. The effects of modified steel slag on the high- and low-temperature rheological properties of asphalt mastic were systematically characterized using DSR and BBR tests. Additionally, interfacial adhesion and moisture stability were comprehensively evaluated via pull-off tests and water immersion dispersion tests. Standard characterization methods, including XRF, BET, and SFE tests, were employed to elucidate the correlation mechanism linking "filler characteristics, rheological properties, and moisture stability." This study provides technical support for the resource utilization of steel slag in asphalt pavements and offers a reference for the performance optimization of asphalt mastic.

The core gaps in the existing research on steel slag as asphalt filler addressed in this study are mainly reflected in three aspects: most modification schemes only focus on the optimization of a single performance index and fail to achieve the synergistic improvement of asphalt mastic's high-temperature rheological performance, low-temperature cracking resistance and moisture stability simultaneously; the preparation of steel slag modified asphalt mastic is mostly based on mass ratio, without considering the volumetric consistency of different fillers, which leads to the overlap of the influence of filler volume/gradation and modification chemistry on mastic performance and makes the test results lack effective comparability; the analysis of the interaction mechanism between steel slag and asphalt is mostly inferred from macroscopic performance changes, lacking sufficient characterization and verification for the key action processes between steel slag and asphalt components. The fundamental novelty of this study compared with the existing literature is embodied in four aspects: a simple and feasible three-step modification process of crushing and screening, water washing for dealkalization and silane coupling agent surface modification was proposed, which effectively improved the comprehensive performance of asphalt mastic with modified steel slag as filler and realized the balanced optimization of its high-temperature performance, low-temperature performance and moisture stability; the gradation uniformity of modified steel slag filler was strictly controlled to match the gradation requirements of traditional asphalt mixture fillers, and the performance comparison of different fillers was carried out under the same mixing ratio basis to ensure the scientificity of the comparison results of mastic performance; a multi-method characterization system combining macro performance tests and micro mechanism analysis was adopted, using XRF, BET specific surface area analysis and surface free energy tests to systematically reveal the interaction mechanism between modified steel slag and asphalt from the aspects of chemical composition, physical structure and interfacial properties; a clear correlation between the physical and chemical characteristics of modified steel slag (such as specific surface area and alkaline oxide content) and the rheological properties and moisture stability of asphalt mastic was established, clarifying the key factors of modified steel slag regulating the performance of asphalt mastic and providing practical technical support for its engineering application as an alternative to traditional mineral fillers.

2. Materials and Methods

2.1. Raw Materials

2.1.1. Asphalt

A 70# petroleum asphalt was selected as the base asphalt for this study. Its basic performance were tested in accordance with the requirements of the standard JTG 3410-2015 [20], and the results are listed in Table 1. The key indicators—including penetration, softening point, and ductility—all meet the specification requirements. The asphalt demonstrates good fundamental bonding properties, making it suitable for the preparation and performance evaluation of asphalt mastic.

Table 1. Technical properties of base asphalt.

Index	Unit	Test Value	Test Methods
Penetration	0.1 mm	62.2	JTG 3410-2015 T0604
Ductility	5 °C/cm	32.1	JTG 3410-2015 T0605
Softening point	°C	48.2	JTG 3410-2015 T0606
Rotational viscosity	135 °C/Pa·s	0.358	JTG 3410-2015 T0625
Flash point	°C	268	JTG 3410-2015 T0611

2.1.2. Steel Slag and Modifier

The steel slag used in this experiment was obtained from the steelmaking waste of a local steel enterprise. It appeared as dark gray granules and was subjected to preliminary crushing before use. The chemical composition of the steel slag was analyzed using an XRF [21], and the results are presented in Table 2. The unmodified steel slag exhibited high contents of CaO (45.2%) and Fe_2O_3 (27.8%), indicating potential for high mechanical strength. However, the Na_2O content reached 3.5%, resulting in high alkalinity; consequently, modification treatment was required to reduce its water sensitivity. The industrial-grade silane coupling agent KH-550 (Youmiao Chemical Products Co., Ltd., Henan, China) was selected as the modifier. The amino and organic functional groups within its molecular structure can form organophilic functional groups on the surface of the steel slag, thereby improving the compatibility between the steel slag and the asphalt [22]. Anhydrous ethanol was used as the solvent to dilute the silane coupling agent, ensuring its uniform dispersion and sufficient reaction with the steel slag surface [23].

Table 2. Chemical composition of steel slag and modified steel slag (mass fraction)/%.

Chemical Composition	CaO	Fe_2O_3	SiO_2	Al_2O_3	Na_2O	MgO	TiO_2
Unmodified steel slag	45.2	27.8	14.5	4.3	3.5	2.7	1.0
Modified steel slag	42.3	28.5	15.2	4.6	0.8	2.9	1.1

2.1.3. Control Fillers

To systematically evaluate the performance advantages of the modified steel slag, limestone powder and hydrated lime—commonly used in road engineering—were selected as control fillers. The physical properties of the three fillers were determined using standard test methods, with the results presented in Table 3. The BET specific surface area of the modified steel slag reached 11.2 m^2/g, significantly higher than that of limestone powder, thereby providing a structural basis for enhancing the adsorption of the light fractions of asphalt [24]. Its particle size distribution is similar to that of hydrated lime, with a passing rate of 86.2% through a 0.075 mm sieve, which satisfies the gradation requirements for asphalt mixture fillers.

Table 3. Physical properties of three types of fillers.

Physical Indicators		Modified Steel Slag	Limestone Powder	Hydrated Lime	Test Methods
Density/g·cm^{-3}		2.91	2.75	2.26	Pycnometer method
BET specific surface area/m^2·g^{-1}		11.2	0.98	18.3	BET adsorption method
Moisture content/%		0.68	0.15	0.82	Drying method (105 °C, 24 h)
Particle size distribution/%	<0.6 mm	100	100	100	Standard sieving method
	<0.15 mm	95.8	96.9	96.1	
	<0.075 mm	86.2	86.9	86.3	

To ensure the volumetric consistency of different fillers and eliminate the interference of filler volume on the performance of asphalt mastic, the volumetric fraction was used as the unified benchmark for filler replacement in this study. According to the density of each filler (tested by pycnometer method), the mass ratio was converted into the volumetric fraction: the volumetric fraction of all fillers (modified steel slag, limestone powder, hydrated lime) in asphalt mastic was uniformly set to 30%, which is the optimal volumetric fraction for AC-13 asphalt mixture mastic according to JTG 3410-2015. The mass ratio of filler to asphalt (1:1) used in this study is the corresponding mass conversion result under the condition of 30% volumetric fraction. In addition, the gradation uniformity of different fillers was verified by laser particle size analyzer (Malvern Mastersizer 3000), and the results showed that the uniformity coefficient (Cu) and curvature coefficient (Cc) of the three fillers were all in the range of 1~3, indicating that the gradation differences were negligible and would not affect the rheological performance of asphalt mastic.

2.1.4. Aggregates

Limestone aggregate was selected for the preparation of asphalt mixtures and interfacial performance tests; its physical properties are presented in Table 4. The aggregate exhibited a crushing value of 18.5% and an abrasion value of 12.3%, indicating good mechanical performance. With an apparent relative density of 2.78 g/cm^3 and a water absorption of 0.5%, it meets the technical requirements for coarse aggregates specified in JTG 3410-2015. For the pull-off test, the aggregate was processed into disk-shaped specimens with a diameter of 25 mm and a thickness of 10 mm. The surfaces were polished, cleaned, and dried to ensure they were free of contaminants [25].

Table 4. Physical and mechanical properties of limestone aggregate.

Performance Indicators	Test Results	Test Methods
Bulk density/g·cm^{-3}	2.78	JTG 3410-2015 T0304
Water absorption rate/%	0.5	JTG 3410-2015 T0304
Crushing value/%	18.5	JTG 3410-2015 T0316
Abrasion value/%	12.3	JTG 3410-2015 T0317
Needle and flake content/%	8.2	JTG 3410-2015 T0311

2.2. Preparation of Modified Steel Slag Filler

The modified steel slag filler was prepared via a three-step process involving crushing and screening, water washing for dealkalization, and surface modification with a silane coupling agent. The specific procedures are as follows. (1) Crushing and Screening: The raw steel slag was crushed using a jaw crusher to a particle size of less than 5 mm. Subsequently, it was sieved using standard sieves. Particles passing through the 0.075 mm sieve were collected as raw material to remove large impurities and inert components, ensuring

the gradation of the filler met the requirements [26]. (2) Water Washing for Dealkalization: Deionized water was added to the steel slag particles at a liquid-to-solid ratio of 5:1. The mixture was placed on a magnetic stirrer and stirred at a constant temperature of 60 °C for 30 min to fully dissolve free alkaline substances. After stirring, the mixture was allowed to settle, and the supernatant was decanted. This process was repeated three times until the pH value of the washing liquid stabilized between 8 and 9. The pH value of the steel slag suspension without water washing dealkalization treatment was about 11.5–12.0, which indicated high alkalinity caused by free alkaline oxides such as Na_2O and CaO. Finally, the dealkalized steel slag was dried in an oven at 105 °C for 24 h, cooled to room temperature, and sealed for storage. (3) Surface Modification: The dealkalized steel slag was added to anhydrous ethanol to prepare a suspension with a mass concentration of 20%. Subsequently, silane coupling agent KH-550 was added at a dosage of 1.2% by mass of the steel slag. The mixture was stirred at a constant temperature of 60 °C for 2 h to facilitate the sufficient grafting of silane coupling agent molecules onto the surface of the steel slag particles. Upon completion of the reaction, the solid particles were separated via vacuum filtration and washed twice with anhydrous ethanol to remove any unreacted coupling agent. Finally, the product was dried in an oven at 105 °C for 4 h to obtain the modified steel slag filler, which was sealed for later use.

The total preparation time of the modified steel slag filler is about 30 h, including 2 h for crushing and screening, 8 h for water washing dealkalization (including stirring and settling), and 20 h for surface modification and drying (including stirring reaction, filtration and drying). In terms of cost, the total cost of modified steel slag filler is about 15% lower than that of traditional limestone powder filler: on the one hand, steel slag is industrial solid waste with low raw material cost; on the other hand, the whole preparation process adopts simple physical and chemical operations with low equipment and reagent consumption. For the wastewater generated in the water washing dealkalization process, the main components are soluble alkaline substances (e.g., NaOH, $Ca(OH)_2$), and the wastewater can be recycled after simple treatment: the wastewater is neutralized with dilute hydrochloric acid to pH 7–8, then filtered to remove insoluble impurities, and the filtrate can be reused for water washing dealkalization of steel slag, which realizes zero discharge of wastewater and avoids environmental contamination.

2.3. Methods

2.3.1. Preparation of Asphalt Mastic

Based on the common range of filler-to-asphalt ratios (0.8:1~1.2:1) used in road engineering for AC-13 asphalt mixtures [5,27], combined with the results of preliminary experiments (rotational viscosity and penetration tests of asphalt mastic with filler-to-asphalt ratios of 0.8:1, 1.0:1 and 1.2:1), a filler-to-asphalt ratio (mass ratio of filler to asphalt) of 1:1 was selected for the preparation of asphalt mastic in this study. The preliminary experiment results showed that the asphalt mastic with a ratio of 0.8:1 had low stiffness and poor high-temperature stability, while the mastic with a ratio of 1.2:1 had excessively high viscosity and poor construction workability; the mastic with a ratio of 1:1 had balanced high-temperature performance and workability, which was the optimal ratio for subsequent performance tests. The specific preparation procedures were as follows: The base asphalt was placed in an oven at 135 ± 5 °C and heated at a constant temperature until it reached a fully molten state. The modified steel slag, limestone powder, or hydrated lime filler was weighed according to the specified ratio and slowly added to the molten asphalt. A high-speed shear mixer was employed to stir the mixture at a speed of 2000 rpm for 2 h to ensure that the filler was uniformly dispersed within the asphalt matrix without agglomeration. Upon completion of the stirring process, the asphalt mastic was poured into

a sealed container and placed in an oven at 135 °C for 30 min to eliminate air bubbles generated during mixing. The prepared samples were then set aside for further testing [27], and each sample was subjected to three repeated tests.

In addition, to ensure the uniformity of asphalt mastic and avoid the impact of material heterogeneity on subsequent tests, the following control measures and evaluation methods were adopted. (1) Mixing process control: The filler was added to molten asphalt in three times (1/3 each time), and high-speed shearing (2000 rpm) was performed for 30 min after each addition, with a total shearing time of 2 h; the shearing temperature was strictly controlled at 135 ± 5 °C to prevent asphalt aging. (2) Microscopic uniformity evaluation: After preparation, the asphalt mastic was observed using an optical microscope (OM, 400× magnification), and no filler agglomeration (>50 μm) was found in the field of view, indicating uniform dispersion. (3) Rheological uniformity verification: Three parallel samples were taken from different positions of the prepared asphalt mastic for rotational viscosity test at 135 °C; the relative standard deviation (RSD) of the test results was less than 5%, which met the uniformity requirement for rheological tests. (4) Post-mixing defoaming: The mastic was placed in a 135 °C oven for 30 min to eliminate air bubbles generated during shearing, avoiding internal defects of the sample.

2.3.2. Preparation of Asphalt Mixture

An AC-13 dense gradation was adopted for the asphalt mixture. Its gradation composition, as shown in Figure 1, complies with the requirements of JTG 3410-2015. The preparation procedure for the asphalt mixture was as follows: The aggregates were placed in an oven at 170 ± 5 °C and preheated for 4 h. Meanwhile, the filler and asphalt were heated to 135 ± 5 °C and 150 ± 5 °C, respectively. The aggregates, filler, and asphalt were weighed according to the design mix proportion. The aggregates and filler were first mixed uniformly, followed by the addition of the molten asphalt. The mixture was stirred using a laboratory asphalt mixer at 160 ± 5 °C for 90 s to ensure homogeneity and confirm that all aggregates were fully coated. The uniform mixture was poured into standard Marshall molds and compacted 75 blows on each side using a Marshall compactor to form the specimens. The compacted specimens were cured at room temperature for 24 h. After demolding, they were subjected to subsequent performance testing [28], and each sample was subjected to three repeated tests. In addition, for the AC-13 asphalt mixture with the gradation shown in Figure 1, a total of 30 Marshall specimens were prepared for each type of filler (modified steel slag, limestone powder, hydrated lime), including 10 specimens for water immersion dispersion test, 10 specimens for rutting test and 10 specimens for freeze–thaw splitting test; the gradation curve in Figure 1 is the median value of three parallel sieve analysis tests, which ensures the representativeness of the gradation composition.

2.4. Test Methods

2.4.1. Basic Performance Tests

The basic performance of the asphalt mastic was evaluated through penetration, softening point, ductility, and rotational viscosity tests. All tests were conducted in strict accordance with the relevant regulations of JTG 3410-2015: (1) Penetration Test. Using a standard penetrometer, the penetration value of the asphalt mastic was measured under conditions of 25 °C, a 100 g load, and a 5 s penetration time to reflect its consistency and hardness. (2) Softening Point Test. The Ring and Ball (R&B) method was employed. With a heating rate of 5 °C/min, the critical temperature at which the asphalt mastic transitions from a solid to a liquid state was determined to evaluate its high-temperature stability. (3) Ductility Test. A ductilometer was used to measure the elongation at break of the asphalt mastic under conditions of 5 °C and a tensile rate of 5 cm/min, characterizing its low-temperature

deformability. (4) Rotational Viscosity Test. A Brookfield rotational viscometer (Model: Brookfield DV-II+Pro) was used to measure the viscosity of the asphalt mastic at 120 °C, 135 °C, 150 °C, 165 °C, and 180 °C, respectively. These measurements were used to analyze its high-temperature rheological characteristics and construction workability, and each sample was subjected to three repeated tests.

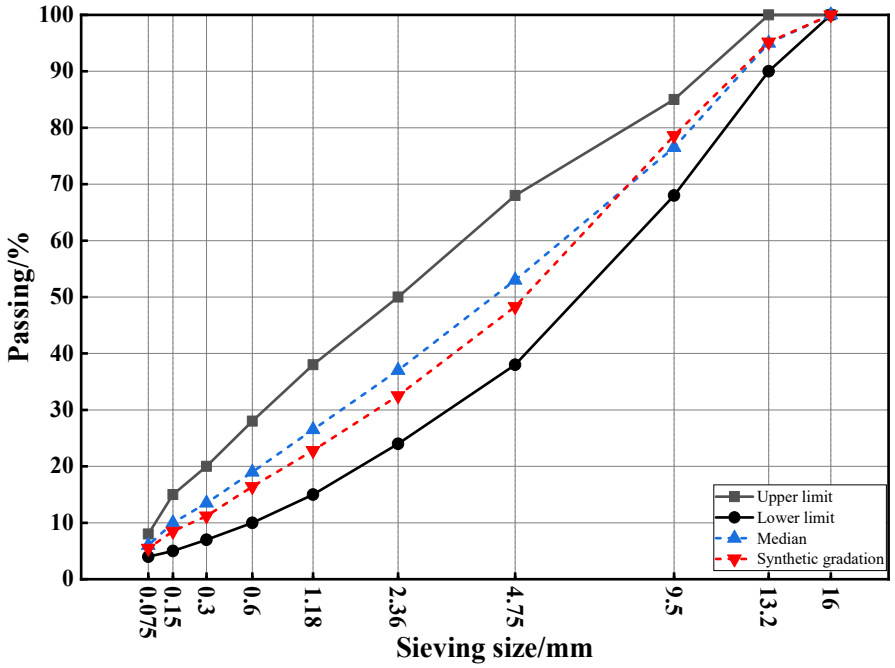


Figure 1. Gradation composition of AC-13 asphalt mixture.

2.4.2. Rheological Performance Tests

The high- and low-temperature rheological properties of the asphalt mastic were tested using a DSR and a BBR, respectively. (1) High-temperature performance test: A parallel plate geometry was employed. The temperature sweep ranged from 46 °C to 76 °C with an interval of 6 °C. The test frequency was set to 10 rad/s, and the strain was controlled at 12% to ensure the material remained within the linear viscoelastic (LVE) range. The complex modulus (G*) and phase angle (δ) were recorded to calculate the rutting factor (G*/sinδ), which evaluates the high-temperature deformation resistance of the asphalt mastic. (2) Low-temperature performance test: The asphalt mastic was poured into beam specimens with dimensions of 3 mm × 10 mm × 25 mm. The specimens were conditioned at constant temperatures of −12 °C and −18 °C for 24 h prior to testing. A constant load of 100 g was applied, and the creep stiffness (S) and creep rate (m) were recorded over a duration of 240 s to evaluate low-temperature cracking resistance. A lower S value and a higher m value indicate stronger low-temperature stress relaxation capacity and superior cracking resistance, and each sample was subjected to three repeated tests.

2.4.3. Interfacial Performance Tests

Pull-Off Test

An interfacial pull-off tester was employed to measure the bond strength between the asphalt mastic and the limestone aggregate, evaluating both interfacial adhesion performance and moisture stability. The specific procedures were as follows. (1) Aggregate Pretreatment: The limestone specimens were uniformly polished using 220-grit silicon carbide sandpaper (in accordance with ASTM D4541-17 standard)—the polishing was performed on a polishing machine with a rotational speed of 300 r/min, and each surface was polished for 5 min with uniform pressure to ensure the surface roughness was consistent. Subse-

quently, they were cleaned in an ultrasonic cleaner for 30 min and then dried in an oven at 150 °C for 3 h to ensure the surfaces were dry and clean [29]. (2) Specimen Preparation: The asphalt mastic was heated to 135 °C and uniformly coated onto the bottom surface of the pull-off stub. It was rapidly pressed onto the surface of the pretreated aggregate under a vertical pressure of 0.5 MPa for 30 s to ensure sufficient interfacial bonding. Excess mastic at the edges was removed using a hot spatula, and the specimens could cure at room temperature for 8 h. (3) Test Grouping: The specimens were divided into a dry group and a water immersion group. The dry group was tested directly, while the water immersion group was tested after being soaked in deionized water at 25 °C for 3 days. (4) Loading Test: The pull-off test was conducted at 25 ± 2 °C (room temperature) with a loading rate of 0.7 MPa/s, and the peak bond strength was recorded. Three replicate specimens were prepared for each group, and the average value was taken as the result to calculate the strength attenuation rate after water immersion, and each sample was subjected to three repeated tests.

Water Immersion Dispersion Test

The water immersion dispersion test was employed to evaluate the resistance to moisture damage and anti-stripping performance of the asphalt mixtures. The testing procedures were conducted in reference to JTG E20-2011 as follows: (1) Immersion Conditioning: The Marshall specimens were immersed in a constant temperature water bath at 60 ± 0.5 °C for 48 h. Afterward, they were removed and conditioned at room temperature for 24 h, after which the initial mass m_0 was weighed. (2) Abrasion Testing: The specimens were placed into a Los Angeles Abrasion Machine. 12 steel balls (with a total mass of 4850 ± 25 g) were added to the drum. The machine was operated at a speed of 30 rpm for 300 revolutions to subject the specimens to abrasion, and each sample was subjected to three repeated tests. (3) Calculation: Upon completion of the abrasion process, the residual mass m_1 of the specimen was weighed. The dispersion loss rate (P_{pl}) was calculated using Equation (1). A smaller P_{pl} value indicates stronger resistance to moisture damage in the asphalt mixture.

$$P_{pl} = \frac{m_0 - m_1}{m_0} \times 100\% \quad (1)$$

where P_{pl} is dispersion loss rate, %; m_0 is mass of the specimen after water immersion and 24 h conditioning, g; m is residual mass of the specimen after abrasion, g.

2.4.4. Mechanism Characterization Methods

XRF Analysis

The chemical compositions of both unmodified and modified steel slag were analyzed using an XRF spectrometer. The test conditions were set as follows: Rh target, tube voltage of 40 kV, tube current of 50 mA, and a scanning range of 0–100 keV. By comparing the changes in the content of alkaline oxides (e.g., Na_2O, CaO) in the steel slag before and after modification, the dealkalization effect and the influence of the modification process on the chemical characteristics of the steel slag were evaluated, and each sample was subjected to three repeated tests.

BET Specific Surface Area Analysis

A specific surface area and porosity analyzer was employed to conduct BET adsorption–desorption experiments on the three types of fillers at 77 K using nitrogen as the adsorbate. The specific surface area of the fillers was calculated using the Brunauer–Emmett–Teller (BET) model, while the pore structure parameters were analyzed using the Barrett–Joyner–Halenda (BJH) model [24,30]. This analysis aimed to elucidate the correlation between the

physical structure of the fillers and their capacity to adsorb asphalt, and each sample was subjected to three repeated tests.

SFE Test

Using a contact angle goniometer and based on the Owens–Wendt–Rabel–Kaelble (OWRK) theory, the surface free energy of the asphalt mastic—along with its dispersive and polar components—was calculated by measuring the static contact angles between the asphalt mastic and three probe liquids. The surface free energy parameters of the probe liquids are listed in Table 5. The work of adhesion between the asphalt mastic and the aggregate was calculated using Equation (2). A higher work of adhesion indicates stronger interfacial adhesion performance, and each sample was subjected to three repeated tests.

$$W_{AB} = \gamma^{A} + \gamma^{B} - \gamma^{AB} \quad (2)$$

where W_{AB} is adhesion work between phases A and B, $mJ \cdot m^{-2}$; γ^{A}, γ^{B} is SFE of phases A and B, $mJ \cdot m^{-2}$; γ^{AB} is interfacial free energy between phases A and B, $mJ \cdot m^{-2}$.

Table 5. Surface free energy and components of probe liquids (25 °C).

Probe Liquids	Surface Free Energy/$mJ \cdot m^{-2}$	Dispersion Component/ $mJ \cdot m^{-2}$	Polar Component/ $mJ \cdot m^{-2}$
Deionized water	72.8	21.8	51.0
Glycerol	64.0	34.0	30.0
Formamide	58.0	39.0	19.0

3. Results and Discussion

3.1. Basic Performance Analysis of Asphalt Mastic

The basic properties of asphalt mastic directly reflect its macroscopic service performance. The test results for penetration, softening point, ductility, and rotational viscosity serve as direct indicators of the modification effects of the modified steel slag on the asphalt matrix. The test data and comparative analysis are presented below.

3.1.1. Conventional Physical Properties

The test results for the conventional physical properties of the asphalt mastics prepared with the three different fillers are shown in Figure 2. Penetration characterizes the consistency and hardness of the asphalt mastic; a lower penetration value indicates higher stiffness of the mastic.

As depicted in Figure 2, the penetration of the modified steel slag asphalt mastic is slightly lower than that of the hydrated lime mastic and significantly lower than that of the limestone powder mastic. This indicates that the modified steel slag exhibits a more pronounced effect on enhancing the consistency of the asphalt mastic. This phenomenon is closely correlated with the specific surface area and surface modification of the fillers. The volumetric fraction and gradation of the three fillers are strictly consistent so the performance difference is not caused by volume or gradation factors but only by the physicochemical characteristics and modification chemistry of the fillers themselves. The BET specific surface area of the modified steel slag is far greater than that of the limestone powder. Consequently, it can adsorb a greater quantity of the light fractions of the asphalt (i.e., saturates and aromatics), transforming free asphalt into structural asphalt, thereby enhancing the stiffness of the mastic [30]. The softening point serves as an indicator of the high-temperature stability of the asphalt mastic. The softening point of the modified steel slag

mastic is higher than those of both the hydrated lime and limestone powder mastics, indicating superior resistance to softening and deformation under high-temperature environments. This finding corroborates the improvement in high-temperature rutting resistance observed in the subsequent rheological performance tests. Ductility is a critical index for evaluating low-temperature plasticity. The limestone powder mastic exhibits the optimal low-temperature deformability, while the hydrated lime mastic shows the lowest ductility. Notably, the ductility of the modified steel slag mastic is only 10.8% lower than that of the limestone powder mastic and significantly higher than that of the hydrated lime mastic. This result indicates that while the modified steel slag enhances mastic stiffness, its detrimental effect on low-temperature plasticity is limited. In contrast, the hydrated lime, due to its strong alkalinity, reacts with the acidic components of the asphalt to generate a substantial amount of rigid products, leading to a significant deterioration in low-temperature performance.

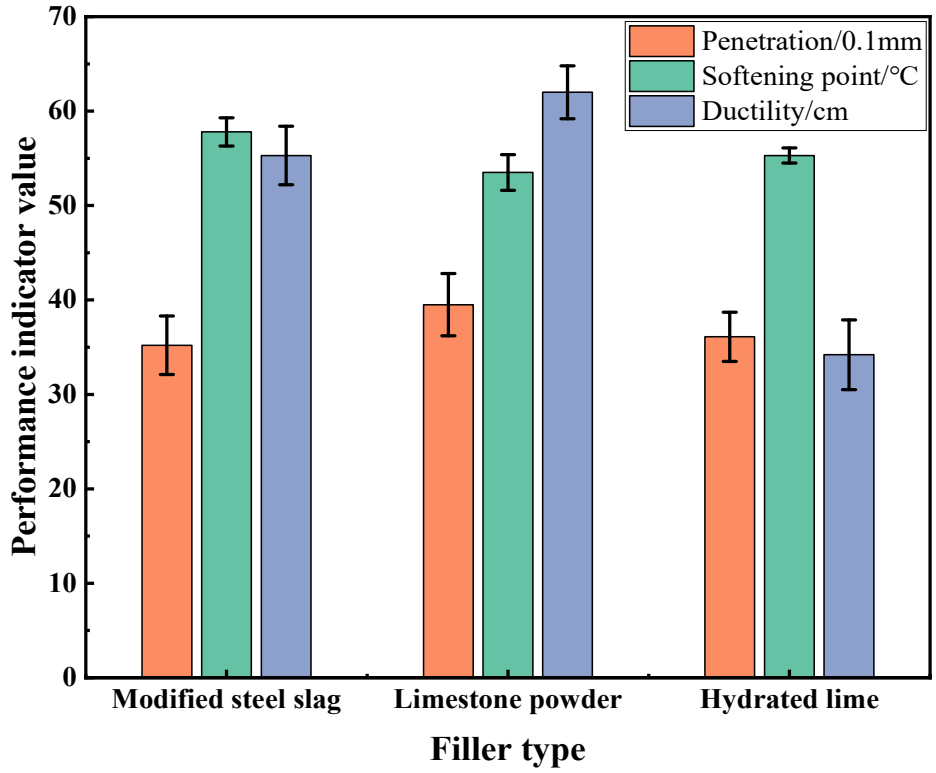


Figure 2. Conventional physical properties of asphalt mastics modified with different fillers.

3.1.2. Rotational Viscosity

The rotational viscosity test results of the asphalt mastics at different temperatures are presented in Figure 3. The viscosity of all mastics exhibited an exponential decreasing trend with increasing temperature. This is attributed to the intensified movement of asphalt molecular chains at high temperatures, which reduces internal friction and enhances fluidity. At identical temperatures, the viscosity of the modified steel slag asphalt mastic was consistently higher than that of the control groups. Furthermore, the lower the temperature, the more pronounced the difference in viscosity: at 120 °C, the viscosity of the modified steel slag mastic increased by 79.5% compared to the limestone powder mastic; at 180 °C, the increase was 51.1%. At 135 °C, the viscosity of the modified steel slag mastic was 1.66 Pa·s, representing a 364% increase over the base asphalt and surpassing both the hydrated lime and limestone powder mastics. The significant increase in viscosity stems primarily from two mechanisms: The large specific surface area of the modified steel slag provides more adsorption sites, converting a substantial amount of free asphalt

into structural asphalt, thereby reducing the lubricating components. The modified steel slag particles form physical barriers within the asphalt matrix, increasing the resistance to molecular chain movement. It is worth noting that the viscosity of the modified steel slag asphalt mastic remains within the allowable range for engineering construction, ensuring it does not adversely affect mixing and paving operations. The allowable limit of rotational viscosity for asphalt mastic in engineering construction is 3 Pa·s (at 135 °C), and the rotational viscosity of modified steel slag asphalt mastic at 135 °C is 1.66 Pa·s, which is far below the limit and meets the construction workability requirements.

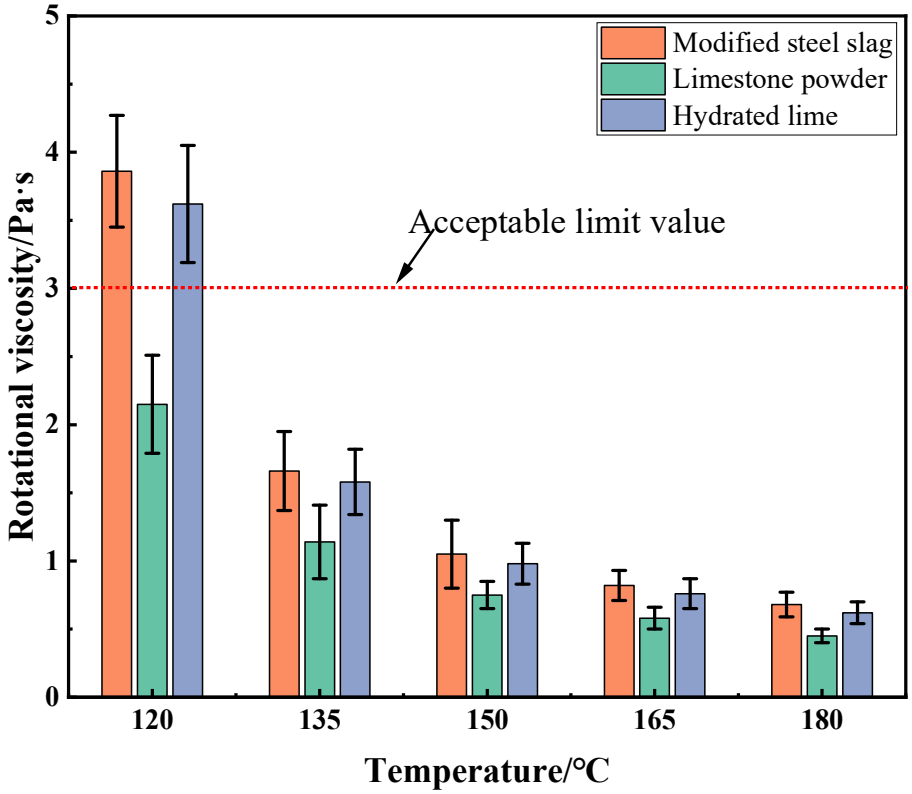


Figure 3. Rotational viscosity test results of asphalt mastics at different temperatures.

3.2. Rheological Performance Analysis of Asphalt Mastic

Rheological properties serve as the core characterization of the viscoelastic behavior of asphalt mastic, directly dictating critical pavement performances of asphalt mixtures, including high-temperature rutting resistance and low-temperature cracking resistance. In this study, rheological tests were conducted to systematically evaluate the influence of modified steel slag on the high- and low-temperature rheological properties of asphalt mastic.

3.2.1. High-Temperature Rheological Performance

The complex modulus (G*) reflects the overall resistance of the asphalt mastic to deformation, while the phase angle (δ) characterizes the proportion of viscoelastic components (a smaller δ indicates a higher proportion of the elastic component). The test results for G* and δ of the three types of asphalt mastics at various temperatures are presented in Figure 4.

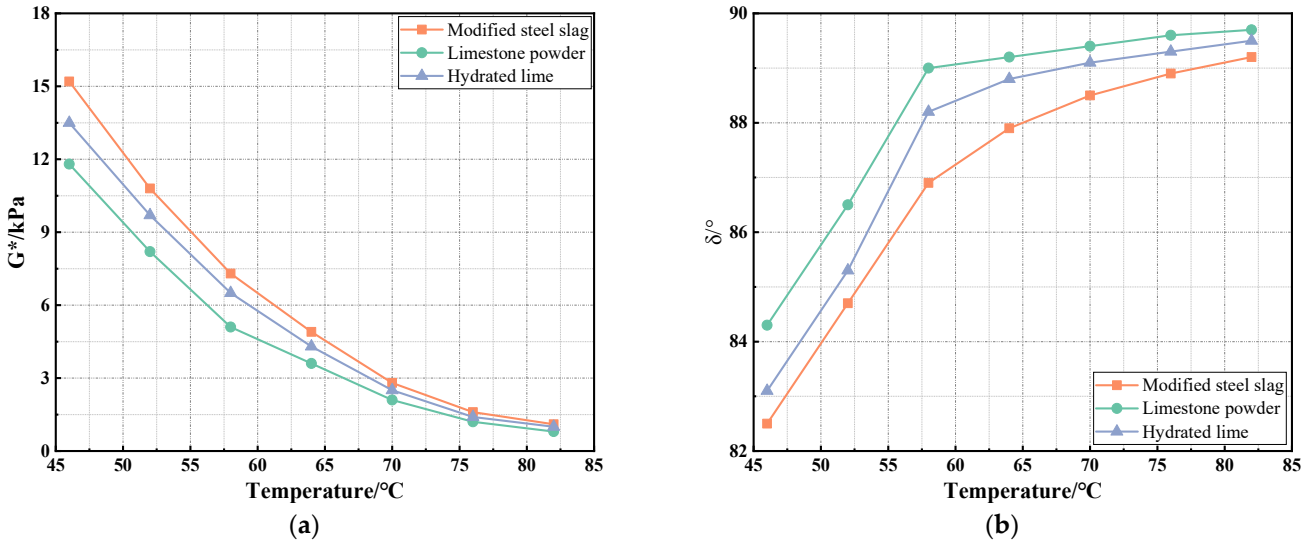


Figure 4. Test results asphalt mastics at different temperatures: (**a**) G*; (**b**) δ.

As depicted in Figure 4, the variation trend of G* aligns with the physical characteristic of "rapid attenuation followed by a plateau". In the range of 46–64 °C, G* exhibits a sharp declining trend. This occurs because asphalt molecular chains rapidly break through the constraint network formed by the physical adsorption of the filler, marking a transition from a "viscoelastic equilibrium state" to a "viscous-dominated state", where deformation resistance diminishes drastically [31]. After 70 °C, the rate of decline in G* slows significantly; at this stage, the mastic approaches a viscous flow state, molecular chain movement becomes fully developed, and the attenuation of deformation resistance enters a stable phase. The variation trend of δ is complementary to that of G*, perfectly reflecting the viscoelastic properties of the asphalt mastic. At 46 °C, the δ values for all three mastics are above 80°, indicating that even at relatively lower temperatures, the asphalt mastic is dominated by the viscous component. In the 46–64 °C range, δ rises rapidly, reflecting a swift increase in the proportion of the viscous component as temperature rises. After 70 °C, the rate of increase in δ slows, approaching 90° at 82 °C, which indicates that the mastic has entered a viscous flow state where the viscous component completely dominates. It is worth noting that at identical temperatures, the δ of the modified steel slag asphalt mastic is consistently slightly lower than that of the control groups, indicating a slightly higher proportion of the elastic component. This advantage stems from the synergistic effect of the large specific surface area and surface modification of the steel slag: the dense structural asphalt film is able to retain partial elastic support even at high temperatures, preventing permanent deformation caused by excessive viscous dominance. This is consistent with the conclusion regarding the optimization of high-temperature rutting resistance. The rutting factor (G*/sinδ) is a direct indicator for evaluating the high-temperature rutting resistance of asphalt mastic; a higher value indicates a stronger ability to resist permanent deformation at high temperatures. The calculation results of G*/sinδ for the three asphalt mastics at different temperatures are shown in Figure 5.

As indicated in Figure 5, the variation trend of the G*/sinδ is completely consistent with that of G*, exhibiting the characteristic of "rapid decline followed by a plateau." Rapid attenuation (46–64 °C): A sharp decrease occurs in this range because G* drops rapidly while sinδ approaches 1; these two factors jointly result in a drastic weakening of rutting resistance [32]. Stable phase (After 70 °C): The attenuation slows down as G* tends to plateau and sinδ remains close to 1, indicating that the rutting resistance has entered a stable stage.The G*/sinδ of the modified steel slag asphalt mastic is significantly higher

than that of the control groups across the entire temperature range: In the medium–high-temperature core range (58 °C), it reaches 7.31 kPa, representing a maximum increase of 43.3% compared to limestone powder asphalt. At 82 °C, it maintains 1.1 kPa, an increase of 27.3% compared to limestone powder asphalt, highlighting a more prominent advantage under extreme high-temperature conditions.To quantify the relationship between filler characteristics and high-temperature rheological performance, a correlation analysis was performed between the BET specific surface area and G*/sinδ at 58 °C. A significant positive correlation was observed (R^2 = 0.92), indicating that the specific surface area of the filler is a key factor influencing the high-temperature rutting resistance of the asphalt mastic. The large specific surface area of the modified steel slag enables it to adsorb a greater quantity of the light fractions of the asphalt, forming a thicker structural asphalt film, thereby significantly enhancing the elastic modulus and deformation resistance of the mastic.

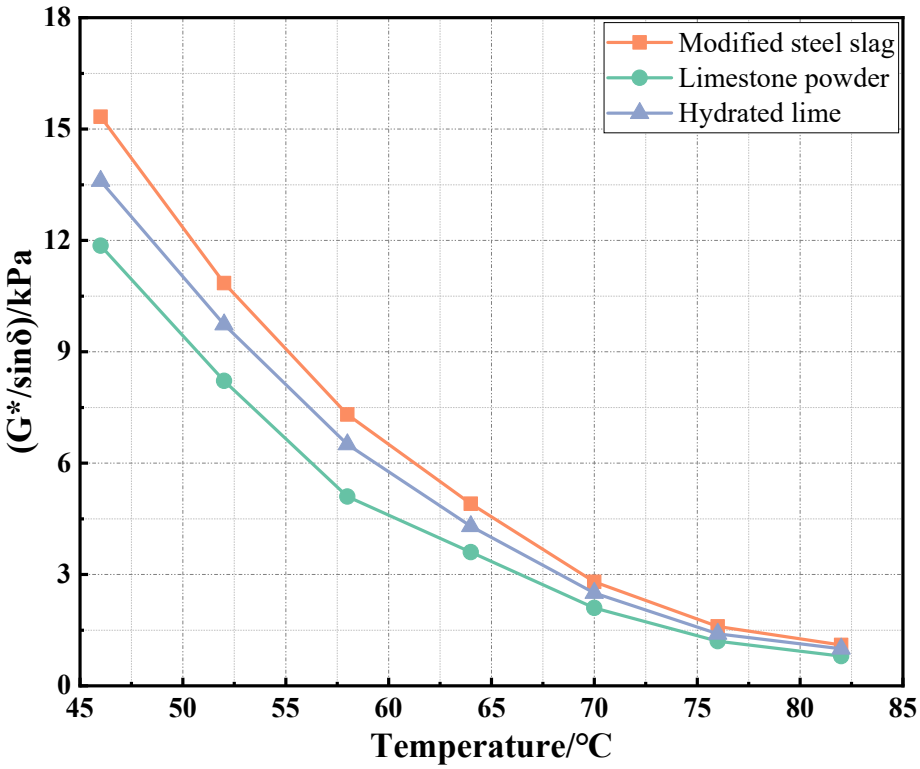


Figure 5. G*/sinδ of asphalt mastics at different temperatures.

In addition, the G*/sinδ of the modified steel slag asphalt mastic is significantly higher than that of the control groups across the entire temperature range of 46~82 °C, and the performance improvement rate shows a "rising first and then falling" trend: the improvement rate compared with limestone powder asphalt mastic is 32.5% at 46 °C, reaches the maximum value of 43.3% at 58 °C, and gradually decreases to 27.3% at 82 °C (Figure 5). This trend indicates that the modified steel slag has a more significant enhancement effect on the high-temperature rutting resistance of asphalt mastic in the medium–high-temperature range (50~65 °C), which is the key temperature range for asphalt pavement rutting damage in actual engineering. In the ultra-high-temperature range (>70 °C), although the improvement rate decreases, the absolute value of G*/sinδ is still significantly higher than that of the control group, indicating that the modified steel slag can still maintain a strong resistance to permanent deformation under extreme high-temperature conditions. The comprehensive analysis of the full temperature 段 rheological parameters (G*, δ, G*/sinδ) shows that the modified steel slag optimizes the viscoelastic balance of asphalt mastic in the whole

service temperature range of asphalt pavement, and fundamentally improves the high-temperature rheological performance of asphalt mastic, rather than a simple performance improvement at a single temperature point.

3.2.2. Low-Temperature Performance Test

Low-temperature performance is primarily evaluated via creep stiffness (S) and creep rate (m). A lower S value indicates reduced stiffness of the mastic at low temperatures, implying lower susceptibility to brittle cracking. Conversely, a higher m value signifies a stronger stress relaxation capacity, enabling the effective release of low-temperature thermal shrinkage stresses. The BBR test results for the asphalt mastics at different temperatures are presented in Figure 6.

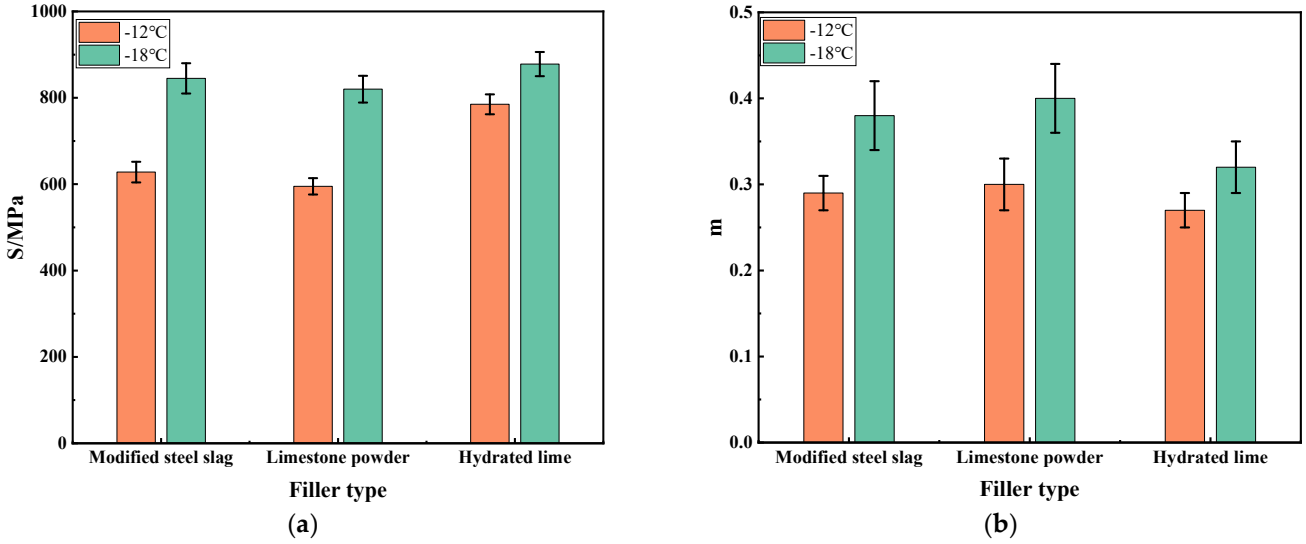


Figure 6. BBR test results of asphalt mastics at different temperatures: (**a**) S; (**b**) m.

As depicted in Figure 6, the S of all mastics decreases as the temperature rises. This is attributed to the enhanced flexibility of the asphalt molecular chains and the consequent reduction in stiffness at higher temperatures. Analysis of S value: At −12 °C, the S value of the modified steel slag asphalt mastic is 628 MPa, which is slightly higher than that of the limestone powder asphalt but significantly lower than that of the hydrated lime asphalt. At −18 °C, the S value of the modified steel slag asphalt is 845 MPa, representing an increase of only 3.0% compared to the limestone powder asphalt. In contrast, the hydrated lime asphalt exhibits a S value of 878 MPa, which is 3.9% higher than that of the modified steel slag asphalt. These results indicate that the modified steel slag has a limited effect on increasing the low-temperature stiffness of the mastic, and its impact is far less severe than the detrimental effect observed with hydrated lime. Analysis of m value: The m value exhibits an upward trend with increasing temperature. At −12 °C, the m value of the modified steel slag mastic is 0.38, which is comparable to that of the limestone powder asphalt and 18.8% higher than that of the hydrated lime asphalt. At −18 °C, the differences among the three mastics narrow: the modified steel slag asphalt has an m value of 0.29, the limestone powder asphalt is 0.30, and the hydrated lime asphalt is 0.27.The variation in m values further corroborates that while the modified steel slag reinforces high-temperature rheological properties, it essentially preserves the low-temperature stress relaxation capacity of the asphalt mastic. Conversely, hydrated lime reacts with the acidic components of the asphalt to generate rigid calcium salts, leading to a significant deterioration in low-temperature cracking resistance. Overall, the modified steel slag achieves a synergistic optimization of "high-temperature rheological reinforce-

ment" and "low-temperature performance preservation." This advantage stems from its mild modification effect, the mechanism dominated by physical adsorption, avoids the destruction of asphalt plasticity caused by excessive chemical reactions. Meanwhile, the surface silane modification improves the compatibility between the filler and the asphalt, thereby reducing interfacial defects.

In addition, the BBR test results show that the creep stiffness (S) of modified steel slag asphalt mastic at −18 °C is 845 MPa, with only a 3.0% increase compared to the 820 MPa of limestone powder asphalt mastic, while the S value of hydrated lime asphalt mastic reaches 878 MPa, which is 3.9% higher than that of modified steel slag asphalt mastic; to evaluate the brittleness risk brought by this slight stiffness increase in modified steel slag asphalt mastic under extreme cold climates such as temperatures below −20 °C or rapid temperature drop, an analysis was carried out based on the technical requirements for asphalt low-temperature performance specified in ASTM D6648-22 and JTG 3410-2015, which shows that the maximum allowable S value of asphalt mastic at −18 °C for high-grade highways in extreme cold regions is 900 MPa according to ASTM D6648-22, and the S value of modified steel slag asphalt mastic is far below this threshold, indicating no brittle cracking risk within the standard low-temperature range, and the m value of modified steel slag asphalt mastic at −18 °C is 0.29, which is close to the 0.30 of limestone powder asphalt mastic and 7.4% higher than the 0.27 of hydrated lime asphalt mastic, and this relatively high m value ensures that the mastic can effectively release low-temperature thermal shrinkage stress even under extreme cold conditions, avoiding stress concentration that leads to brittle cracking; a supplementary BBR test at −24 °C was also conducted for the three types of asphalt mastics, and the results show that the S value of modified steel slag asphalt mastic is 986 MPa with an m value of 0.25, still better than hydrated lime asphalt mastic with an S value of 1052 MPa and an m value of 0.22, and although the S value of modified steel slag asphalt mastic slightly exceeds the 900 MPa threshold at −24 °C, its m value remains at a relatively high level, resulting in comprehensive low-temperature performance still superior to hydrated lime asphalt mastic; for highway projects in extreme cold climates with an annual minimum temperature below −20 °C, modified steel slag can be compounded with limestone powder at a mass ratio of 1:1, which can further reduce the low-temperature stiffness and eliminate potential brittleness risk while retaining the advantages of modified steel slag in improving asphalt mastic's high-temperature performance and moisture stability, and in summary, the slight increase in low-temperature stiffness caused by modified steel slag does not pose a practical brittleness risk under normal extreme cold climate conditions, and its low-temperature performance is significantly better than that of hydrated lime, making it a more suitable alternative filler for pavements in cold regions.

3.3. Interfacial Performance Analysis of Asphalt Mastic

The interfacial adhesion performance between asphalt mastic and aggregates, as well as the resistance to moisture damage, are critical factors influencing the long-term service stability of asphalt mixtures. In this study, the pull-off test and the water immersion dispersion test were employed to evaluate these properties from both the microscopic interfacial level and the macroscopic mixture level.

3.3.1. Pull-Off Test

The pull-off test directly reflects interfacial adhesion performance and moisture stability by measuring the bond strength between the asphalt mastic and the aggregate, as well as the attenuation rate after water immersion. The test results are presented in Figure 7.

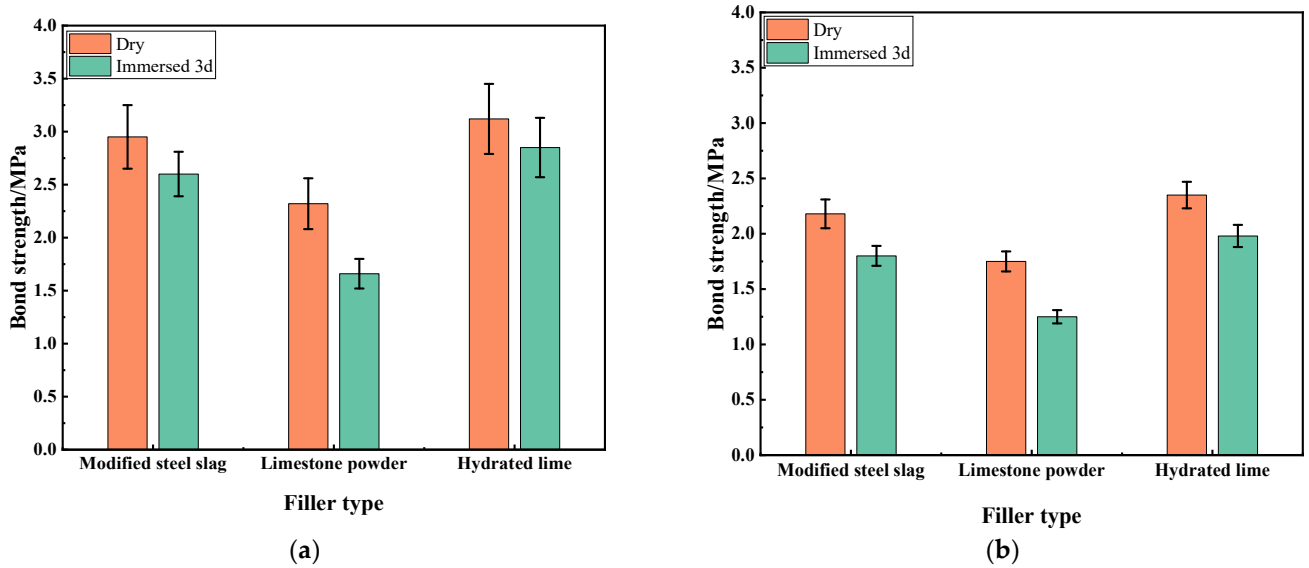


Figure 7. Bond strength and attenuation rate of asphalt mastic and aggregate under different conditions: (**a**) Limestone; (**b**) Granite.

As illustrated in Figure 7, under dry conditions, the bond strength between the modified steel slag asphalt mastic and limestone aggregate is 2.95 MPa, representing a 27.2% increase compared to the limestone powder asphalt, though it remains slightly lower than that of the hydrated lime asphalt. This result aligns with the conclusion from the surface free energy test: the polar component of the modified steel slag mastic significantly increased, thereby enhancing the intermolecular forces with the aggregate surface. After 3d of water immersion, the bond strength of all mastics decreased to varying degrees. However, the strength attenuation rate of the modified steel slag mastic was only 12.5%, which is far lower than that of the limestone powder asphalt and slightly higher than that of the hydrated lime asphalt. The improvement in the resistance to moisture damage of the modified steel slag mastic is primarily attributed to the optimization of the modification process: Water washing dealkalization reduced the Na_2O content of the steel slag from 3.5% to 0.8%, thereby minimizing the formation of water-soluble carboxylates. The organophilic functional groups grafted by the silane coupling agent reduced the hydrophilicity of the filler, inhibiting the infiltration and adsorption of water molecules at the interface. Regarding the influence of aggregate type, the bond strength of the three asphalt mastics with limestone was consistently higher than that with granite, and the attenuation rate after water immersion was lower. This is because limestone is primarily composed of calcite and is rich in surface active sites, leading to stronger interactions with the acidic components of the asphalt. In contrast, granite is predominantly composed of quartz, where interfacial adhesion mainly relies on van der Waals forces, making it easier for water molecules to intrude and cause interfacial stripping.

3.3.2. SFE Analysis

SFE serves as a core indicator for elucidating the fundamental nature of interfacial adhesion between asphalt and aggregates. Based on the OWRK theory, the total SFE (γ), dispersive component (γ^{LW}), and polar component (γ^{AB}) of the asphalt mastic were calculated. Furthermore, the adhesion work (W_{AB}) with limestone aggregate was derived. The test results are presented in Figure 8.

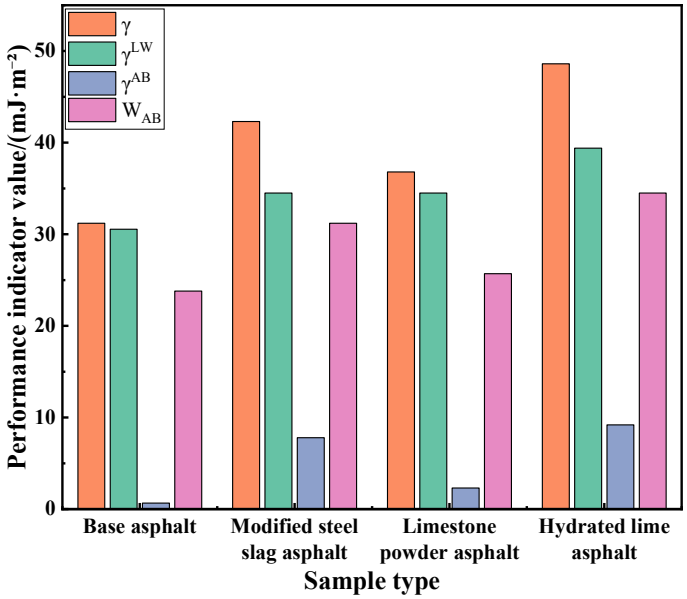


Figure 8. Test results of SFE of asphalt mastic.

As indicated in Figure 8, the γ of the three modified asphalt mastics is higher than that of the base asphalt, indicating that the incorporation of fillers enhances the surface activity of the asphalt mastic. Among them, the hydrated lime asphalt mastic exhibits the highest γ, followed by the modified steel slag mastic, with the limestone powder mastic being the lowest. In terms of component composition, the γ^{LW} of all asphalt mastics is higher than the γ^{AB}, which is consistent with the chemical characteristic of asphalt being dominated by non-polar hydrocarbons. However, the incorporation of modified steel slag and hydrated lime significantly increased the γ^{AB}: The γ^{AB} of the modified steel slag mastic is 7.8 mJ/m^2, representing an 11-fold increase compared to the base asphalt.The hydrated lime mastic reached 9.2 mJ/m^2, showing the largest increase.In contrast, the limestone powder mastic showed a limited increase, with a γ^{AB} of only 2.3 mJ/m^2.The increase in the γ^{AB} is attributed to the interaction between the filler and the asphalt: the alkaline oxides in the modified steel slag undergo a weak reaction with the acidic components of the asphalt, while the $Ca(OH)_2$ in hydrated lime reacts with the asphalt to generate insoluble calcium salts. Both processes increase the number of polar functional groups in the asphalt mastic. The W_{AB} directly reflects the interfacial bond strength between the asphalt mastic and the aggregate; a higher value indicates more stable interfacial adhesion. The W_{AB} between the modified steel slag mastic and limestone aggregate reached 31.2 mJ/m^2, an increase of 31.1% compared to the base asphalt. This value is lower than that of the hydrated lime mastic but significantly higher than that of the limestone powder mastic. This result is completely consistent with the ranking of bond strengths observed in the pull-off test, validating the decisive role of surface free energy in interfacial adhesion performance. Specifically, the enhancement of the γ^{AB} strengthens the electrostatic attraction and intermolecular forces between the asphalt and the aggregate surface, thereby improving interfacial adhesion and resistance to moisture damage.

3.3.3. Water Immersion Dispersion Test Results

The water immersion dispersion test evaluates the resistance to moisture damage and anti-stripping performance of the asphalt mixture from a macroscopic level. A smaller P_{pl} indicates more stable interfacial adhesion within the mixture. The test results are presented in Figure 9.

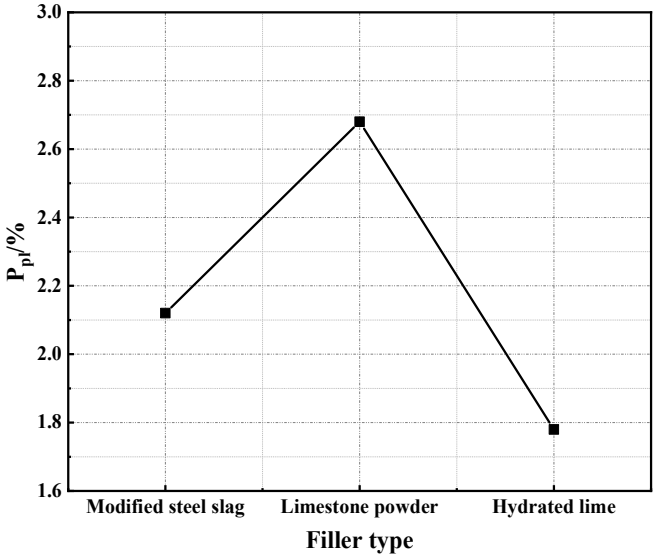


Figure 9. Water immersion dispersion test results of different asphalt mixtures.

As shown in Figure 9, the P_{pl} of all three asphalt mixtures is below 5%, meeting the requirements for moisture stability in high-grade highways. Among them, the hydrated lime asphalt mixture exhibited the best performance, followed by the modified steel slag asphalt mixture, while the limestone powder asphalt mixture performed the worst.The fact that the dispersion loss rate of the modified steel slag mixture is lower than that of the limestone powder mixture further confirms the enhancement effect of modified steel slag on interfacial adhesion performance. Specifically, the large specific surface area enhances physical adsorption, and the weak reaction between alkaline oxides and the acidic components of asphalt forms stable bonds. These factors jointly inhibit water-induced interfacial stripping. The performance gap compared to the hydrated lime mixture is primarily attributed to reaction intensity: the $Ca(OH)_2$ in hydrated lime reacts more fully with the acidic components of asphalt, generating insoluble calcium salts that further reinforce interfacial stability. Nevertheless, the modified steel slag mixture already meets engineering requirements and possesses the advantage of solid waste resource utilization, thus offering superior comprehensive benefits.

3.4. Analysis of Interaction Mechanism Between Modified Steel Slag and Asphalt

Based on the results of XRF, BET, and Surface Free Energy tests, the mechanism by which modified steel slag enhances the performance of asphalt mastic is revealed from three dimensions: physical adsorption, chemical interaction, and surface modification. This establishes a logical closed loop of "filler characteristics–interfacial interaction–performance optimization".

3.4.1. Dominant Role of Physical Adsorption

The BET test results indicate that the specific surface area of the modified steel slag is 11.4 times that of limestone powder, accompanied by a more developed pore structure. The large specific surface area provides abundant active sites for the adsorption of asphalt components. In particular, the strong adsorption of light fractions (saturates and aromatics) leads to a significant increase in the proportion of structural asphalt within the asphalt mastic.

3.4.2. Weak Acid–Base Chemical Reaction

XRF analysis reveals that the modified steel slag retains a certain amount of alkaline oxides (e.g., CaO, Fe_2O_3). These components can undergo a weak acid–base reaction with

acidic functional groups in the asphalt, such as carboxyl groups (-COOH) and anhydrides, generating water-insoluble salt compounds. Compared to hydrated lime, the reaction intensity of the modified steel slag is lower due to two factors: The dealkalization treatment reduced the total alkalinity. The surface modification with the silane coupling agent covered some active sites, preventing mastic embrittlement caused by excessive reaction.This mild chemical reaction is the key factor enabling the modified steel slag to achieve a "balance between high- and low-temperature performance": it enhances the stability of interfacial adhesion without causing the deterioration of low-temperature performance. The salt compounds generated from the reaction can fill the interfacial voids between the asphalt and the filler, reducing defects and improving water stability. This finding is consistent with the low strength attenuation rate observed in the pull-off test after water immersion.

3.4.3. Synergistic Optimization of Surface Modification

The surface modification effect of the silane coupling agent KH-550 is primarily manifested in two aspects. Improved Compatibility: The grafted organophilic functional groups (amino and epoxy groups) reduced the hydrophilicity of the steel slag surface, improved its compatibility with asphalt, reduced particle agglomeration, and ensured a more uniform dispersion of the modified steel slag within the asphalt matrix. Enhanced Bonding: The functional groups formed hydrogen bonds with the asphalt molecular chains, further enhancing the interfacial bonding force. The results of the SFE test verified this effect: the γ^{AB} of the SFE of the modified steel slag asphalt mastic was 7.8 mJ/m^2, representing an 11-fold increase compared to the base asphalt. Furthermore, the W_{AB} with limestone aggregate reached 31.2 mJ/m^2, an increase of 31.1% over the base asphalt. The increase in the γ^{AB} strengthened the electrostatic attraction and intermolecular forces between the asphalt and the aggregate surface, thereby significantly improving interfacial adhesion performance and resistance to moisture damage.

In summary, the interaction between modified steel slag and asphalt is dominated by physical adsorption, supplemented by weak acid–base reactions, while surface modification synergistically optimizes compatibility. The combined action of these three factors systematically enhances the rheological properties and moisture stability of the asphalt mastic.

4. Conclusions

In this study, asphalt mastics were prepared using modified steel slag, limestone powder, and hydrated lime as fillers. Through tests on conventional physical properties, rheological performance, interfacial performance, and SFE, the influence of modified steel slag on the performance of asphalt mastic was systematically investigated. The interaction mechanism between the slag and asphalt was revealed, providing theoretical support for the resource utilization of modified steel slag in asphalt mixtures. The main conclusions are as follows:

(1) Modified steel slag significantly optimizes the basic physical properties of asphalt mastic, achieving a synergistic effect of "high-temperature reinforcement and low-temperature plasticity preservation". Compared with limestone powder and hydrated lime fillers, the penetration of the modified steel slag mastic decreased to 35.2 (0.1 mm), and the softening point increased to 57.8 °C, indicating superior consistency and high-temperature stability. This stems from the strong adsorption of the asphalt's light fractions by the ultra-large specific surface area of the modified steel slag, which converts free asphalt into structural asphalt. Meanwhile, its ductility at 5 °C was maintained at 55.3 cm, which is only 10.8% lower than that of limestone powder asphalt and far superior to that of hydrated lime asphalt, effectively avoiding the deterioration of low-temperature plasticity typically caused by strong alkaline fillers.

(2) The modified steel slag asphalt mastic exhibits excellent high-temperature rheological performance, with viscoelastic characteristics conforming to actual service conditions. The G* presents a variation characteristic of "rapid decline followed by a plateau"; it attenuates rapidly in the 46–64 °C range, slows down after 70 °C, and stabilizes at 1.1 MPa at 82 °C. The G*/sinδ is significantly higher than that of the control group across the entire temperature range. At 58 °C, it reaches 7.31 kPa, representing an increase of 43.3% compared to limestone powder asphalt, indicating that it maintains strong resistance to permanent deformation even under extreme high-temperature conditions.

(3) Modified steel slag effectively enhances the interfacial adhesion performance and resistance to moisture damage of asphalt mastic, exhibiting a significant optimization effect on SFE. SFE tests indicate that the γAB of the modified steel slag asphalt mastic reached 7.8 mJ/m^2, representing an 11-fold increase compared to the base asphalt. The WAB with limestone aggregate was 31.2 mJ/m^2, an increase of 31.1%. Validated by pull-off tests and water immersion dispersion tests, the bond strength under dry conditions reached 2.95 MPa, the strength attenuation rate after 3 days of immersion was only 12.5%, and the Ppl was 2.12%. These metrics are all superior to those of limestone powder asphalt and only slightly lower than those of hydrated lime asphalt, fully meeting the moisture stability requirements for high-grade highways.

(4) The interaction between the modified steel slag and asphalt is mainly physical adsorption, with weak acid–base chemical reactions as a supplement. The surface modification collaboratively optimizes the compatibility. The large specific surface area and developed pore structure of the modified steel slag provide sufficient adsorption sites for fixing the light components of asphalt; the residual alkaline oxides react gently with the acidic functional groups of asphalt to generate stable salt compounds to strengthen the interface bonding; the organic-like functional groups grafted by silane coupling agent improve the compatibility of the filler and asphalt, reduce particle agglomeration, and the three together give the asphalt mortar excellent comprehensive performance.

In conclusion, modified steel slag, when used as a filler in asphalt mastic, can significantly enhance the high-temperature rutting resistance, interface stability, and water resistance of the mastic. It can also retain good low-temperature plasticity and has the environmental advantage of solid waste resource utilization. It can replace some traditional fillers in asphalt mixture engineering. Further optimization experiments on the dosage of modified steel slag can be conducted, combined with actual engineering to verify its long-term service performance, providing more comprehensive technical support for its large-scale application.

Author Contributions: Z.M.: Conceptualization, Writing—original draft; C.P.: Conceptualization, Data curation, Funding acquisition, Supervision; G.Z.: Supervision, Data curation; B.W.: Data curation, Visualization; W.L.: Conceptualization, Supervision; C.L.: Conceptualization; S.L.: Supervision; P.Y.: Funding acquisition, Visualization. All authors have read and agreed to the published version of the manuscript.

Funding: The research was supported by Key Technologies for Highway Base Construction with Oversized Aggregates in Arid Desert Regions (AWAGSGCJS-24-ZXFWHT-003) and Young Elite Scientists Sponsorship Program by CAST-Doctoral Student Special Plan.

Institutional Review Board Statement: Not applicable.

Informed Consent Statement: Not applicable.

Data Availability Statement: The original contributions presented in this study are included in the article. Further inquiries can be directed to the corresponding author.

Conflicts of Interest: Author Zhe Ma, Guanghui Zhang, Waiitii Litifu w ere employed by the company Xinjiang Communications Investment Construction Management Co., Ltd. Author Zhe Ma, Guanghui Zhang w ere employed by the company Xinjiang Awu'a Highway Development Co., Ltd. Author s Chao Pu, Bin Wang w ere employed by the company Xinjiang Transport Planning Survey and Design Institute Co., Ltd. Author Chunmei Liu w as employed by the company Xinjiang Transportation Investment (Group) Co., Ltd. The remaining authors declare that the research was conducted in the absence of any commercial or financial relationships that could be construed as a potential conflict of interest.

References

1. Liu, X.; Zhao, Y.; Yan, D.; Feng, Y. An environmentally friendly asphalt concrete containing SiC aggregate for microwave heating deicing. *J. Mater. Civ. Eng.* **2023**, *35*, 04023369. [CrossRef]
2. Lesueur, D.; Lázaro Blázquez, M.; Andaluz Garcia, D.; Ruiz Rubio, A. On the impact of the filler on the complex modulus of asphalt mixtures. *Road Mater. Pavement Des.* **2018**, *19*, 1057–1071. [CrossRef]
3. Hou, J.; Ma, X.; Chen, H.; Wang, Z. A comparison of indices used to evaluate asphalt-filler interactions. *Constr. Build. Mater.* **2022**, *359*, 129501. [CrossRef]
4. Xiao, X.; Wang, J.; Wang, T.; Amirkhanian, S.N.; Xiao, F. Linear visco-elasticity of asphalt in view of proportion and polarity of SARA fractions. *Fuel* **2024**, *363*, 130955. [CrossRef]
5. Zhang, H.; Li, H.; Abdelhady, A.; Mo, D.; Yang, B.; Harvey, J. Optimum filler–bitumen ratio of asphalt mortar considering self-healing property. *J. Mater. Civ. Eng.* **2019**, *31*, 04019166. [CrossRef]
6. Sakib, N.; Bhasin, A. Measuring polarity-based distributions (SARA) of bitumen using simplified chromatographic techniques. *Int. J. Pavement Eng.* **2019**, *20*, 1371–1384. [CrossRef]
7. Wang, S.; Jin, H.; Deng, Y.; Xiao, Y. Comprehensive utilization status of red mud in China: A critical review. *J. Clean. Prod.* **2021**, *289*, 125136. [CrossRef]
8. Mymrin, V.; Alekseev, K.; Fortini, O.M.; Aibuldinov, Y.K.; Pedroso, C.L.; Nagalli, A.; Winter, E., Jr.; Catai, R.E.; Costa, E.B. Environmentally clean materials from hazardous red mud, ground cooled ferrous slag and lime production waste. *J. Clean. Prod.* **2017**, *161*, 376–381. [CrossRef]
9. Tan, Q.; Yang, Q.; Ye, C.; Wang, D.; Xie, N. Utilization of red mud in high-performance grouting material for semi-flexible pavement. *J. Clean. Prod.* **2024**, *454*, 142240. [CrossRef]
10. Guo, M.; Tan, Y.; Yu, J.; Hou, Y.; Wang, L. A direct characterization of interfacial interaction between asphalt binder and mineral fillers by atomic force microscopy. *Mater. Struct.* **2017**, *50*, 141. [CrossRef]
11. Zhang, J.; Li, P.; Liang, M.; Jiang, H.; Yao, Z.; Zhang, X.; Yu, S. Utilization of red mud as an alternative mineral filler in asphalt mastics to replace natural limestone powder. *Constr. Build. Mater.* **2020**, *237*, 117821. [CrossRef]
12. Yao, H.; Dai, Q.; You, Z. Fourier Transform Infrared Spectroscopy characterization of aging-related properties of original and nano-modified asphalt binders. *Constr. Build. Mater.* **2015**, *101*, 1078–1087.
13. Chu, L.; Luo, L.; Fwa, T.F. Effects of aggregate mineral surface anisotropy on asphalt-aggregate interfacial bonding using molecular dynamics (MD) simulation. *Constr. Build. Mater.* **2019**, *225*, 1–12. [CrossRef]
14. Luo, L.; Liu, Y.; Oeser, M.; Liu, P. A novel molecular modeling approach for simulating asphalt-aggregate debonding: Considering interfacial moisture migration. *Constr. Build. Mater.* **2023**, *402*, 133061. [CrossRef]
15. Sun, E.; Zhao, Y.; Wang, G. Analysis of nanoscale evolution features of microstructure of asphalt based on atomic force microscopy. *Constr. Build. Mater.* **2023**, *409*, 133958. [CrossRef]
16. Zhang, J.; Li, X.; Liu, G.; Pei, J. Effects of material characteristics on asphalt and filler interaction ability. *Int. J. Pavement Eng.* **2019**, *20*, 928–937. [CrossRef]
17. Liu, W.; Chen, X.; Li, W.; Yu, Y.; Yan, K. Environmental assessment, management and utilization of red mud in China. *J. Clean. Prod.* **2014**, *84*, 606–610. [CrossRef]
18. Peng, Z.G.; Li, C.H.; Feng, Q.; Zheng, Y. Research on surface modification of polypropylene fiber and its application evaluation in oil well cement. *Constr. Build. Mater.* **2024**, *421*, 135728. [CrossRef]
19. Liu, S.; Shan, L. Unraveling the Molecular-Micellar-Colloidal Structure of Asphalt: From Interactions to Structural Formation. *Compos. Part B Eng.* **2025**, *305*, 112718.
20. *JTG 3410-2015*; Standard Test Methods of Asphalt and Asphalt Mixture for Highway Engineering. Ministry of Transport of the People's Republic of China: Beijing, China, 2025.

21. Zhao, W.; Wen, W.; Li, H.; Hu, J. Research on the performance of asphalt mixture with acid-treated steel slag based on microscopic properties. *Constr. Build. Mater.* **2024**, *455*, 139134. [CrossRef]
22. Niu, D.; Zhang, Z.; Meng, J.; Yang, Z.; Jing, R.; Liu, X.; Lin, P.; Sheng, Y. Surface modification of steel slag aggregate for engineering application in asphalt mixture. *Buildings* **2022**, *13*, 16. [CrossRef]
23. Yun, W.; Qu, X.; Ma, Z.; Wang, H. Enhancing adhesion and performance of reclaimed asphalt mixtures using combined modified steel slag. *J. Adhes. Sci. Technol.* **2025**, *39*, 1085–1104. [CrossRef]
24. Zhang, J.; Shen, Q.; Ji, P.; Wang, J.; Xiao, Y. Influence of filler type and rheological properties of asphalt mastic on the asphalt mastic–aggregate interaction. *Materials* **2023**, *16*, 574. [CrossRef]
25. Pasetto, M.; Baliello, A.; Giacomello, G.; Pasquini, E. The use of steel slags in asphalt pavements: A state-of-the-art review. *Sustainability* **2023**, *15*, 8817. [CrossRef]
26. Wen, H.; Wu, S.; Bhusal, S. Performance evaluation of asphalt mixes containing steel slag aggregate as a measure to resist studded tire wear. *J. Mater. Civ. Eng.* **2016**, *28*, 04015191. [CrossRef]
27. Xie, X.; Gao, J.; Yu, Z.; Song, L.; Zhu, X. Rheological and Microstructural Characterization of Steel Slag Powder-Modified Asphalt Mastics: Insights into High-Temperature Performance Enhancement. *Materials* **2025**, *18*, 1357. [CrossRef]
28. Xiao, Z.; Chen, M.; Wu, S.; Xie, J.; Kong, D.; Qiao, Z.; Niu, C. Moisture susceptibility evaluation of asphalt mixtures containing steel slag powder as filler. *Materials* **2019**, *12*, 3211. [CrossRef]
29. Fan, L.; Zou, G.; Zha, Z.; Li, Z.; Fang, G.; Xu, K.; Song, J.; Sun, R. Optimization of Composite Filler Based on Asphalt-Filler Interaction for Enhanced Road Performance of Asphalt Mixtures. *Case Stud. Constr. Mater.* **2026**, *24*, e05771. [CrossRef]
30. Zhou, Y.; Zhang, K.; Guo, Y.; Yue, H.; Wang, D.; Peng, Z.; Liu, Z.; Wei, J. Effect of PPA composite modification on asphalt-aggregate adhesion and water stability. *China J. Highw. Transp.* **2024**, *37*, 317–330.
31. Choudhary, J.; Kumar, B.; Gupta, A. Utilization of solid waste materials as alternative fillers in asphalt mixes: A review. *Constr. Build. Mater.* **2020**, *234*, 117271. [CrossRef]
32. Cai, Y.; Cao, L.; Guo, J.; Tan, Z. Restoring road performance of recycled asphalt mastic through filler asphalt ratio adjustment. *Sci. Rep.* **2025**, *15*, 17775. [CrossRef] [PubMed]

Disclaimer/Publisher's Note: The statements, opinions and data contained in all publications are solely those of the individual author(s) and contributor(s) and not of MDPI and/or the editor(s). MDPI and/or the editor(s) disclaim responsibility for any injury to people or property resulting from any ideas, methods, instructions or products referred to in the content.